

## Hydrodynamic investigations of bubbly flow in periodic open cellular structures by ultrafast X-ray tomography

Michael Wagner<sup>1,\*</sup>, Johannes Zalucky<sup>2</sup>, Martina Bieberle<sup>1</sup>, Uwe Hampel<sup>1,2</sup>

<sup>1</sup>Technische Universität Dresden, AREVA Endowed Chair of Imaging Techniques  
in Energy and Process Engineering, 01062 Dresden, Germany

<sup>2</sup>Helmholtz-Zentrum Dresden – Rossendorf, Institute of Fluid Dynamics,  
Bautzner Landstraße 400, 01328 Dresden, Germany

\*corresponding author: Michael.Wagner@hzdr.de

---

**Abstract** Packed bubble columns are common multiphase flow reactor types in chemical engineering. Regarding process efficiency, high mass transfer rates are desirable. Especially, periodic open cell structures (POCS) are supposed to increase the interfacial density and hence the mass transfer in multiphase reactions. At the Helmholtz-Zentrum Dresden – Rossendorf an ultrafast X-ray imaging technique is used to analyze a wide range of multiphase flow scenarios. A rotating electron beam induces X-ray generation on two targets which enables to produce up to 8000 cross-sectional images per second from two measurement planes with a spatial resolution of about 1 mm. We applied this tomography system in an experimental setup including POCS. In the three-dimensional tomography data sets, bubbles were identified and characterized. For different gas flow rates, we determined the axial velocities of the gas-phase, bubble size distributions, bubble aspect ratios and time-averaged gas hold-ups. We compared these results with measurements in an unpacked-bubble column. The results show that the POCS have a significant influence on the hydrodynamics, especially regarding the interfacial area density.

**Keywords:** ultrafast, X-ray CT, two-phase flow, packed bubble column

---

### 1 Introduction

Multiphase flows play a major role in many industrial fields. Especially in chemical engineering, the hydrodynamics of multiphase flows in reactors significantly influence the efficiency and safety of processes. A widely used reactor type is the bubble column [1, 2]. Here, gas is injected at the bottom of a vertical liquid-filled column. In order to increase the process efficiency, columns can be packed with solid structures such as lamellar structures, foams [3, 4] and regular grid structures [5]. These components significantly influence the hydrodynamics within the column. Further, these structures can be coated with catalysts. A structure of special interest is the periodic open cellular structure (POCS) [6] since these are supposed to increase the mass transport at low increase of pressure drop. Therefore, the hydrodynamic investigation of POCS is currently a field of high interest.

The visualization of the flow within structured and conventional bubble columns and the corresponding quantitative evaluation is a demanding challenge. Optical methods such as laser induced fluorescence (LIF) [7] provide detailed images of bubble shapes but require a complex adjustment of refraction indices. Further, this method is only applicable for flow regimes with a limited interfacial density. Therefore, different tomographic measurement techniques have gained increasing interest for studying different kind of bubble columns. Gamma-ray computed tomography [8] provides a high spatial resolution for time-averaged investigations. Furthermore, wire-mesh sensors [9] are used for multiphase flow investigations. These sensors provide high spatial and temporal resolution. Since this technique is invasive, its application is limited to measurements directly below or above the structure but not within.

In the next section, we introduce the ultrafast X-ray tomography system ROFEX, which allows the visualization of multiphase flows with high temporal and spatial resolution within the structure. Further, the experimental setup for the investigation of the hydrodynamics within a POCS is given. The data processing from the detector readings to images with segmented phase distribution is explained in section three. Finally, bubble velocities and bubble size distributions are presented, which are essential hydrodynamic parameters for the characterization of POCS.

## 2 Measurement setup

### 2.1 Ultrafast X-ray tomography system

The Ultrafast X-ray tomography system ROFEX [10] at the Helmholtz-Zentrum Dresden – Rossendorf is a measurement system with two horizontal cross-sectional imaging planes, which are sampled quasi simultaneously. The distance between both planes is 13 mm. The system works with an electron beam gun, which focuses an electron beam with an acceleration voltage of 150 kV on two circular shaped X-ray producing targets. The targets are positioned around the object to be measured. According to the two measurement planes, the detector system consists of two circular rings with a diameter of 216 mm. Both rings are formed by 432 detector pixels. Each pixel has an active area of  $1.3 \text{ mm} \times 1.3 \text{ mm}$ . The geometry allows artefact-free tomography of objects with a diameter of up to 160 mm. A photograph of the system and a principle sketch is given in Fig. 1a. For the tomography scanning, the electron beam is deflected such that a rotating focal spot is produced on the target which generates X-ray radiation penetrating the object within the rings. After every revolution, the focal spot alternates between both target rings. Since there are no moving parts involved in the tomography scanning, this principle allows up to 8000 beam revolutions per second corresponding to the same number of cross-sectional CT images per second. Several phantom studies revealed a spatial resolution of about 1 mm for two-phase flow scenarios.

### 2.2 Measurements of POCS

For the experimental investigation of the POCS we used a DN100 PVC column. Within the column a POCS with a height of 200 mm and a diameter of 98.5 mm was installed (Fig. 1b). The grid of the POCS is formed by bridges with a length of 5 mm and a width of 1 mm. All bridges are exactly arranged in the horizontal plane and perpendicular to it. These bridges envelop cubic-shaped open cells with inner edge length of 4 mm. The POCS is made of synthetics (ABS) with a similar attenuation coefficient as water in order to avoid higher attenuating materials which would decrease the relevant gas-liquid contrast. Therefore, the structure is not visible in a water-filled column. However, its position in the image data can be obtained through a reference measurement of the empty column. The gas is injected by 115 uniformly distributed needles. The lower edge of the structure is positioned 70 mm above the top of the needles. The measurement plane was 60 mm above the lower edge of the structure. Three different flow rates were investigated: 3.6 l/min, 7.2 l/min and 10.8 l/min which correspond to superficial gas velocities of 0.77 cm/s, 1.53 cm/s and 2.30 cm/s. For each case, the flow was scanned with an imaging rate of 1000 fps per ring. From a series of previous multiphase measurements with ROFEX, this scan rate turned out to be high enough for an accurate recognition of bubbles and the determination of its velocities. In order to gain sufficient statistics, the acquisition time for each measurement was set to 10 s. In order to evaluate the obtained hydrodynamic parameters, all measurements were repeated with a POCS-free bubble column.

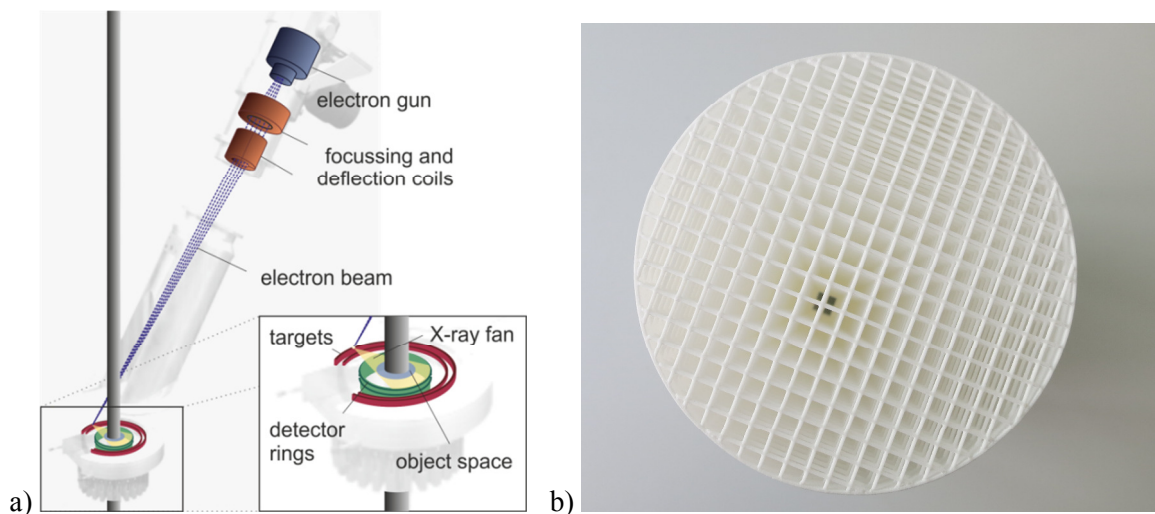


Figure 1: Principle of ultrafast X-ray CT (a), Top-view on the POCS (b).

### 3 Data processing

Each scan provides two stacks (one for each ring) of 10,000 fan-beam sinograms  $I^{(meas)}$  which contain the measured X-ray intensities. According to the attenuation law, one obtains for every beam described by source position  $i$  and detector pixel  $j$  an attenuation value

$$E_{i,j} = \frac{I_{i,j}^{(meas)} - I_j^{(dark)}}{I_{i,j}^{(0)} - I_j^{(dark)}}$$

with  $I_{i,j}^{(0)}$  being a measurement with no object inside the tomography system and  $I_j^{(dark)}$  being the measured detector signal in case of absence of X-rays. Due to required shielding,  $I_{i,j}^{(0)}$  does not represent the original source intensity. Therefore,  $E$  is not the absolute but the relative attenuation sinogram. Afterwards, the sinograms  $E$  are restored as parallel-beam sinograms by a simple resort algorithm based on the geometry of the measurement system. The image reconstruction of these parallel-beam sinograms is performed by filtered back-projection with the Shepp-Logan filter [11]. The resolution of the resulting images is chosen such that the width of one image pixel is 0.5 mm. An example of such a reconstructed gray-scaled image  $\mu_{meas}$  is shown in Fig. 2. The gray values of the images are the relative attenuation coefficients of the different materials. Therefore, calibration of the gas and liquid phase requires a reconstructed image  $\mu_{gas}$  of the emptied column which equals 100% gas and an image  $\mu_{liquid}$  of the water-filled column without gas injection which equals 100% liquid. Then, the scaled image  $\mu_{scaled}$  is given as

$$\mu_{scaled} = \frac{\mu_{meas} - \mu_{gas}}{\mu_{liquid} - \mu_{gas}}$$

With that, the gas peak of the gray value distribution is set to 0 and the liquid peak is set to 1. The scaled sample image is also shown in Fig. 2. In the next step, the gray value image data is binarized by a segmentation algorithm particularly developed for ROFEX image data of gas-liquid flows [12]. This method is based on a stepwise detection of bubbles by pixel agglomeration and shrinking steps. Although the image data is two-dimensional in space, this algorithm works on the complete three-dimensional image stack. The accuracy was investigated by application on phantom data as well as on real two-phase flow data. The results were more accurate compared to other algorithms, such as gradient-based methods, for instance.

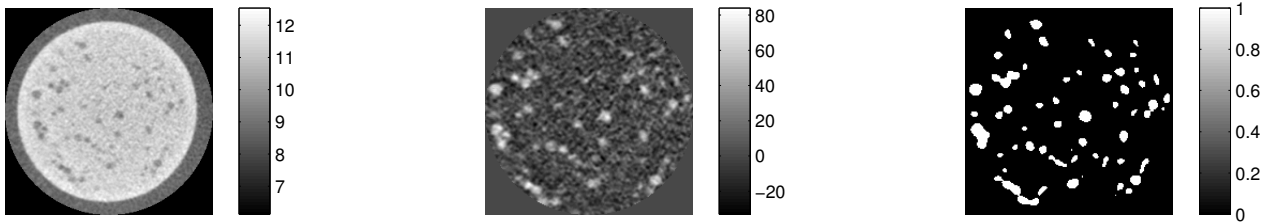


Figure 2: Cross-sectional raw image (left), image after scaling (center) and binarized image (right). The values of the raw image are relative attenuation coefficients. The values of scaled image are given as percentage of the gas phase.

### 4 Results

Based on the segmented image data, the bubble velocities were determined by correlation of the image data of both rings. In case of the investigation of POCS, for each vertical channel of the structure the binary image values are given over time. By correlating these signals of both rings for the same channel, one obtains an average time delay for each channel. This leads to an average bubble velocity for each channel by taking the known vertical distance between both rings into account. In case of POCS-free measurements, the average velocities were determined in ring-shaped regions of the cross-section. In Table 1, the velocities are given for the inner circular region with a diameter of 25 mm. For each gas flow rate, the bubble velocity is significantly lower in the packed column. In general, the determination of single bubble velocities based on the segmented image data is possible but requires sophisticated analysis algorithms, which are able to

reliably cope with the bubble identification problem between both imaging planes. So far, such an algorithm is not yet implemented. However, in order to obtain a characteristic bubble size distribution, the time-averaged velocity is assumed to be accurate enough.

Superficial gas velocity	0.77 cm/s	1.53 cm/s	2.30 cm/s
With POCS	0.22 m/s	0.23 m/s	0.23 m/s
Without POCS	0.28 m/s	0.30 m/s	0.32 m/s

Table 2: Average bubble velocity for the inner region of the bubble column. The diameter of this region is 25 mm.

The calculated bubble velocity allows a spatial scaling of the image data in vertical direction. In Fig. 3, three-dimensional views of the different flows are shown. It is obvious, that the bubble sizes increase with increasing gas flow rate. For quantitative evaluation, the bubble sizes are determined as the sum of the image voxels belonging to one bubble multiplied by the volume of one voxel. In Fig. 4, the bubble size distributions are given for each of the six measurements. The peaks of the histogram of the measurements with POCS show characteristic bubble sizes from 8.1 mm<sup>3</sup> for the lowest gas flow rate up to 18.8 mm<sup>3</sup> for the highest, whereas in case of the unpacked column, the range of the characteristic bubble sizes reaches from 10.1 mm<sup>3</sup> up to 30.5 mm<sup>3</sup>.

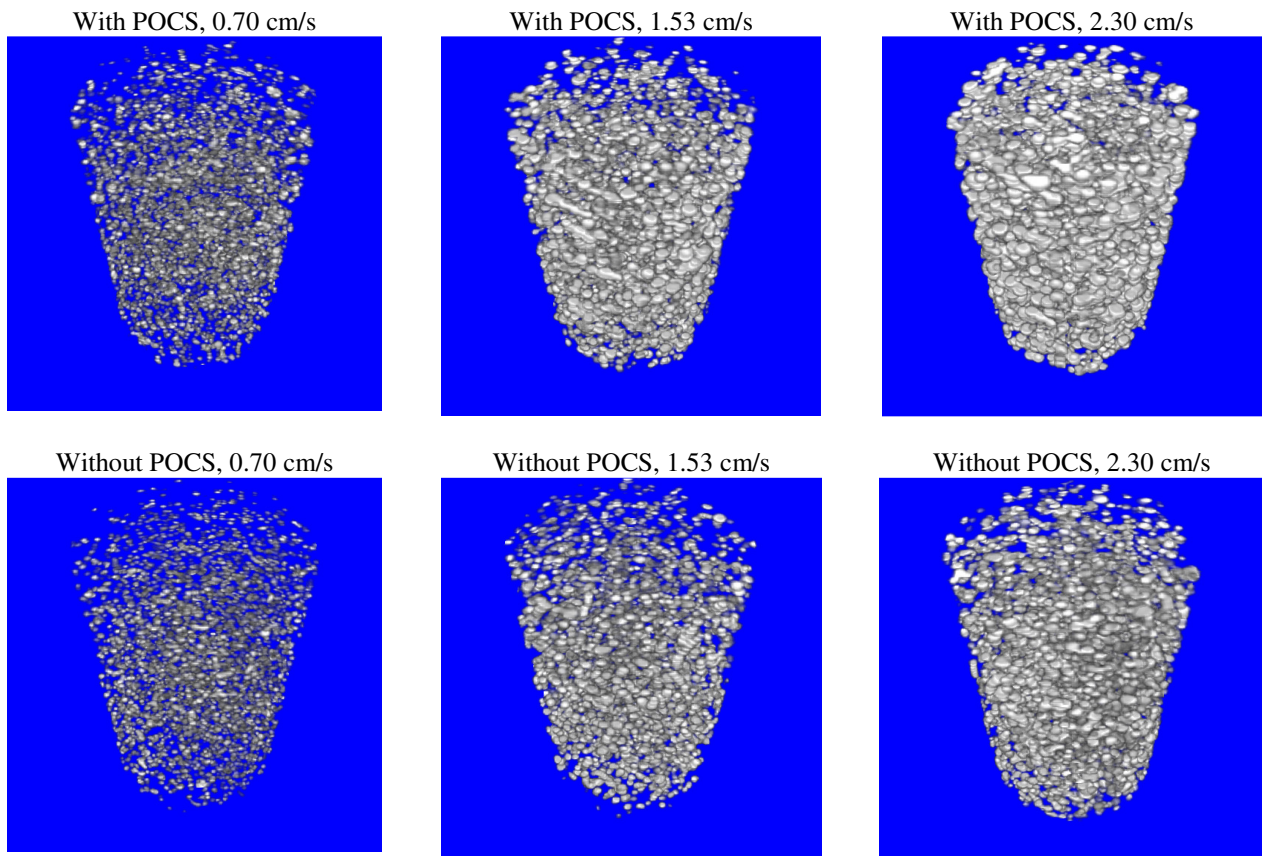


Figure 3: 3D-stack of the binarized image data of the six investigated flow scenarios.

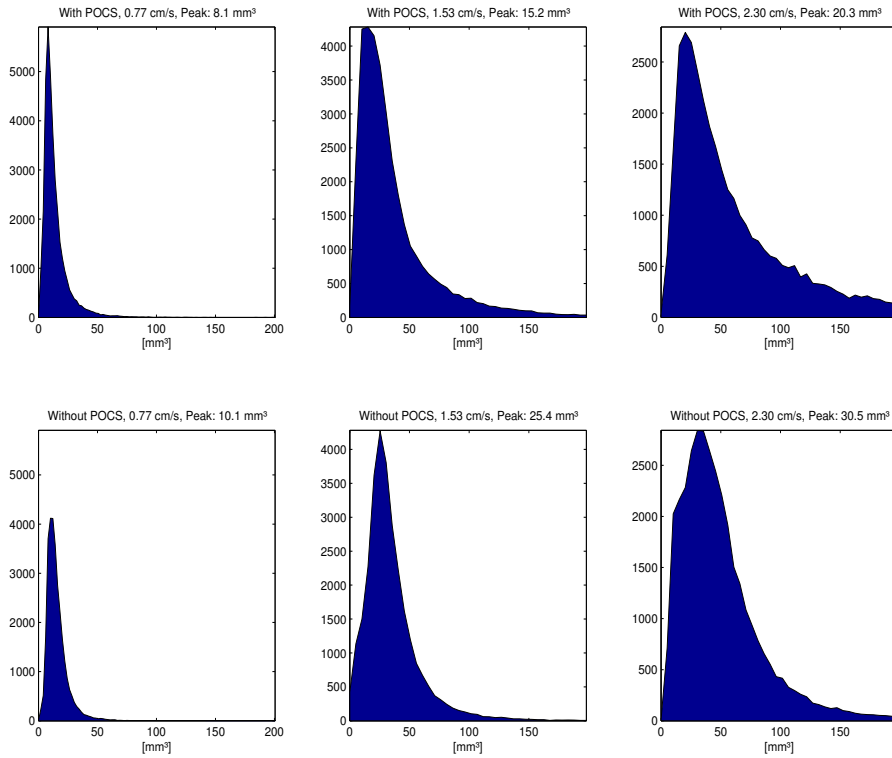


Figure 4: Bubble size distributions of the six investigated flow scenarios.

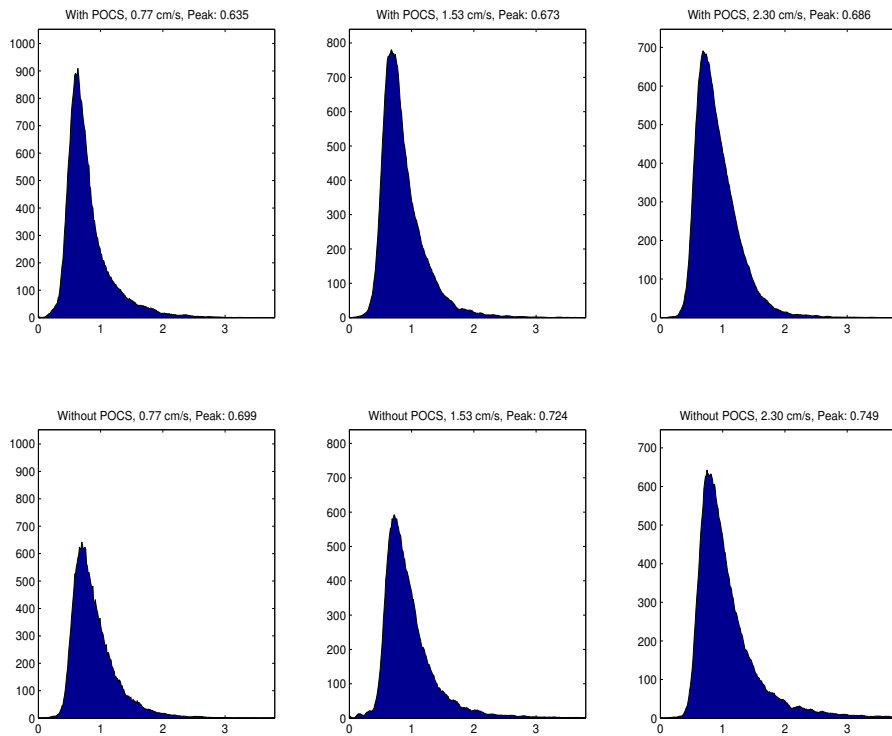


Figure 5: Bubble aspect ratio distributions of the six investigated flow scenarios. The curves are smoothed for better visualization.

For a more detailed view on the bubble shapes, the distributions of the bubble aspect ratio are given in Fig. 5. This parameter is the ratio between the maximal vertical extension of the bubble and its maximum horizontal circle equivalent diameter. Bubbles with a small ratio have a flat shape whereas a ratio near to 1 indicates spherical shape. Although the bubbles in the POCS are smaller than in the unpacked column, Fig. 5 shows that these bubbles are flatter for the lower gas flow rates. Only for the highest gas flow rate, the ratio for the unpacked bubble column is slightly smaller.

Beside these parameters based on the bubble evaluation, it is possible to provide the distribution of the gas hold-up. For this, the segmented image data stack is averaged over time. Fig. 6 shows remarkably higher local and integrated hold-ups within the POCS. Further, the gas is strongly concentrated into the vertical channels.

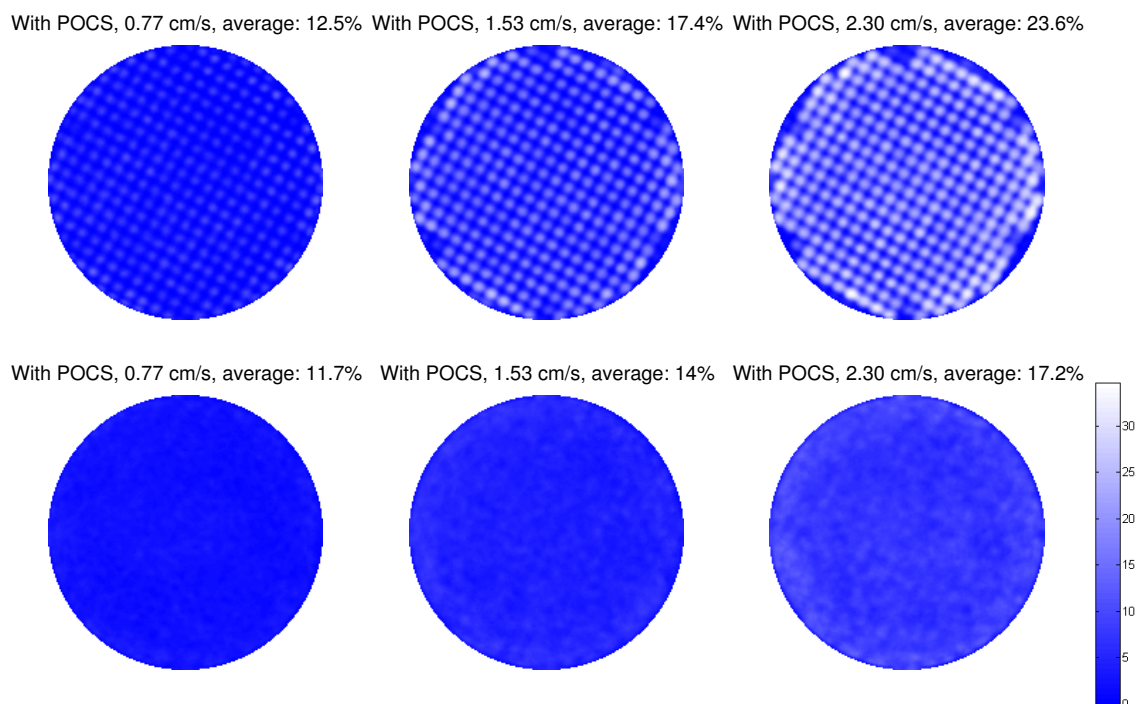


Figure 6: Time-averaged gas hold-up in percentage of the six investigated flow scenarios.

## 5 Conclusion

The ultrafast X-ray tomography system ROFEX allows a detailed investigation of the hydrodynamics of packed bubble columns. Due to its high spatial and temporal resolution, it is possible to visualize the flow regimes, determine hydrodynamic parameters and evaluate the influence of inner structures. The investigated POCS turned out to increase the interfacial area of bubbly flow by forcing the gas to smaller and flatter bubbles compared to the unpacked bubble column. Further, the increased accumulation of gas inside the POCS might positively affect the process efficiency because of the increased interaction between the phases and potential catalysts on the solid structure.

For future work, we plan to extend the data evaluation. In the next steps, single bubble velocities and the exact bubble interfaces will be extracted. Furthermore, the results will be compared with those of other research groups using different measurement techniques. The combined results shall serve as source for creating CFD modelling of such packed bubble columns.

## Acknowledgements

The authors acknowledge the Helmholtz Association for support of the research within the frame of the Helmholtz Energy Alliance 'Energy Efficient Chemical Multiphase Processes'.

## Copyright Notice

The authors waive the terms of the CC license. The content of the paper is subject to the non-exclusive distribution and subsequent publication of this work (e.g., publish a revised version in a journal, post it to an institutional repository or publish it in a book), with an acknowledgement of its initial presentation at this conference.

## References

- [1] Shah, Y. T., Kelkar, B. G., Godbole, S. P., & Deckwer, W. D. (1982). Design parameters estimations for bubble column reactors. *AIChE Journal*, 28(3), 353-379.
- [2] Rabha S, Schubert M (2014) Regime Transition in Viscous and Pseudo Viscous Systems: A Comparative Study. *AIChE Journal*, vol. 60, pp 3079–3090.
- [3] Edouard, D., Lacroix, M., Edouard, D., Lacroix, M., Pham, C., Mbodji, M., & Pham-Huu, C. (2008). Experimental measurements and multiphase flow models in solid SiC foam beds. *AIChE journal*, 54(11), 2823-2832.
- [4] Tschentscher, R., Nijhuis, T. A., Van der Schaaf, J., Kuster, B. F. M., & Schouten, J. C. (2010). Gas-liquid mass transfer in rotating solid foam reactors. *Chemical Engineering Science*, 65(1), 472-479.
- [5] Inayat, A., Schwerdtfeger, J., Freund, H., Körner, C., Singer, R. F., & Schwieger, W. (2011). Periodic open-cell foams: pressure drop measurements and modeling of an ideal tetrakaidecahedra packing. *Chemical Engineering Science*, 66(12), 2758-2763.
- [6] Klumpp, M., Inayat, A., Schwerdtfeger, J., Körner, C., Singer, R. F., Freund, H., & Schwieger, W. (2014). Periodic open cellular structures with ideal cubic cell geometry: Effect of porosity and cell orientation on pressure drop behavior. *Chemical Engineering Journal*, 242, 364-378.
- [7] Bork, O., Schlueter, M., & Raebiger, N. (2005). The Impact of Local Phenomena on Mass Transfer in Gas-Liquid Systems. *The Canadian Journal of Chemical Engineering*, 83(4), 658-666.
- [8] Kemoun, A., Ong, B. C., Gupta, P., Al-Dahhan, M. H., & Dudukovic, M. P. (2001). Gas holdup in bubble columns at elevated pressure via computed tomography. *International Journal of Multiphase Flow*, 27(5), 929-946.
- [9] Da Silva, M. J., Schleicher, E., & Hampel, U. (2007). Capacitance wire-mesh sensor for fast measurement of phase fraction distributions. *Measurement Science and Technology*, 18(7), 2245.
- [10] Fischer, F., & Hampel, U. (2010). Ultra fast electron beam X-ray computed tomography for two-phase flow measurement. *Nuclear Engineering and Design*, 240(9), 2254-2259.
- [11] Kak, A. C., & Slaney, M. (1988). *Principles of computerized tomographic imaging* (Vol. 33). Siam.
- [12] Banowski M, Lucas D, Szalinski L (2015) A new algorithm for segmentation of ultrafast X-ray tomographed gas-liquid flows. *International Journal of Thermal Sciences*, vol. 90, pp 311–322.